Basic study on construction of three-dimensional speed of sound map of excised tissue and evaluation of microscopic characteristics

Genta Hongo[1†], Kazuki Tamura[2], Kazuyo Ito[3], Shinnosuke Hirata[4], Kenji Yoshida[4], and Tadashi Yamaguchi[4*],([1]Grad.Sc.Sci.Eng.,Chiba Univ.; [2]Hamamatsu Univ. School of Medicine.; [3]Tokyo Univ. of Agriculture and Technology.;[4]Center for Frontier Medical Engineering, Chiba Univ.)

1. Introduction

Scanning acoustic microscopy (SAM) equipped with an ultrahigh-frequency ultrasonic sensor can be used to evaluate acoustic properties at the cellular level. However, the relationship between biological tissues and acoustic properties is often studied in two dimensions, and there is concern that this may lead to a discrepancy with diagnosis that reflects the three-dimensional structure of tissues in vivo. In this study, we attempted to understand the correspondence between pathological images and speed of sound (SoS) maps of excised tissues at high resolution by converting them into three-dimensional images.

2 Materials and Methods

2.1 Target materials

Livers from 16-week-old nonalcoholic steatohepatitis (NASH) rat models fed a high-fat diet (HFC, Funabashi Farm) for 10 weeks were used as target tissues in this study. Livers removed from rats were cut into 5 mm square blocks, immersed in formalin for 14 days, fixed, and then paraffin-embedded. Blocks prepared by the paraffin-embedded method were thinly sliced at a thickness of 8 μm and placed on glass slides to prepare 27 thinly sliced specimens.

2.2 Data acquisition

A ZnO transducer (HT-400C, Honda Electronics) with a center frequency of 300 MHz was excited using a pulsar (GZ1120ME-03, GEOZONDAS), and three-dimensional RF echo signals were acquired by scanning the transducer in two dimensions at a scan interval of 2 μm on the top surface of a thin slice sample fixed in a constant-temperature water bath at 23°C. The RF data were recorded by an A/D board (ATS9373, Alazartech) with a sampling frequency of 4 GHz and 12 bit quantization. After ultrasonic measurement, the odd-numbered specimens were HE-stained and the even-numbered specimens were MT-stained, and digital pathology images (1 μm resolution) were acquired by a virtual slide scanner (NanoZoomer S60, Hamamatsu Photonics) to observe tissue structures.

2.3 Speed of Sound analysis

In the three-dimensional RF echo data, the A-mode signal at each measurement point was up-sampled by a factor of 10, and then normalized by the maximum value of each X-axis in the X-Y scan to create an intensity image. After tilt correction in each X-axis, the waveforms were separated by applying an eighth-order autoregressive (AR) model using the echo signal of the glass part selected by Otsu's binarization process as the reference signal, and the speed of sound was calculated from the echoes at the sample surface and back to obtain a two-dimensional SoS map [1)].

2.4 Comparison with pathological histological structures

The intensity image of each sliced specimen acquired in 2.3 was registered between consecutive thin slice samples, and the displacement in each sample was applied to the SoS map of the same sample to construct a three-dimensional SoS map. The pathology image of each sliced specimen was down-sampled so that the number of pixels was equal to the scanning interval of the SoS map, grayscaled, and binarized by Otsu to obtain the shape information of each thin slice sample. Using this shape information, a three-dimensional pathology image was constructed by affine transforming the pathology image so that the Jaccard coefficient between the Intensity image and the pathology image after registration was maximized for each sample, and the shapes of the speed of sound map and pathology image were matched in three dimensions [2)].

The regions of interest (ROIs) of 400 μm × 400 μm were set up in the second MT-stained pathology image (the fourth thin slice of the entire specimen) for the fiber-rich area and the fat droplet-rich area, and the speed of sound was evaluated within each ROI.

[†]g_hongo@chiba-u.jp, [*]yamaguchi@faculty.chiba-u.jp

3. Results and Discussion

An example MT-stained image is shown in **Figure 1(a-1)**, and the SoS map of the same sample is shown in **Figure 1(b-1)**. The red and blue boxes indicate areas containing many fibers and fat, respectively. As a macroscopic structure, the areas with high speed of sound are distributed in a mesh-like pattern throughout the sample, and these can be confirmed as blue-stained fibers in the MT-stained image. In **Figs. 1(a-2)** and **Figs. 1(b-2)**, which are three-dimensional pathological images and three-dimensional SoS maps of the red-framed area, the macroscopic mesh-like structure in Fig. 1(b-1) contains many finer three-dimensional continuous mesh-like structures, which correspond to the fiber structure. In **Figs. 1(a-3)** and **Figs. 1(b-3)**, which correspond to the blue frames, there are many spherical areas with slow speed of sound, which correspond to the fat droplets in the pathological image, which can be confirmed from a microscopic and three-dimensional viewpoint. Since fat is melted during paraffin embedding, the speed of sound values on the sound image do not indicate the nature of fat. On the other hand, microstructures such as cell nuclei could not be captured on the SoS map, and the texture of the SoS map was discontinuous in some areas. This is because the scan interval of the two-dimensional scanning was set to 2 μm to shorten the measurement time, and it was separately confirmed that the speed of sound of the cell nucleus can be independently evaluated with a finer scan interval.

The mean and standard deviation of the speed of sound for the entire region of all samples within the red and blue frames and for the fibrous portion of the MT-stained samples are shown in the box-and-whisker diagram in **Figure 2**. Values of speed of sound less than 1,480 m/s were excluded as glassy areas (including melted fat droplets), and values greater than 1,900 m/s were excluded as outliers. It is assumed that specific tissues can be evaluated stably because the speed of sound of the fibrous part is high and the standard deviation is small compared to the mean and standard deviation of the speed of sound of the entire sample.

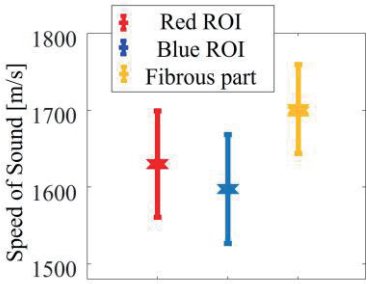

Fig. 2 Speed of sound of NASH rat livers.

4. Conclusion

It was confirmed that three-dimensional registration of pathological images and SoS maps is possible based on the intensity image acquired by SAM, and that it is possible to understand the microscopic speed of sound of microstructures such as fibrous tissue and fat droplets. In this study, the speed of sound of fat droplets could not be evaluated due to the paraffin-embedded thin slice samples were used as the target objects. In the current study, frozen sections, in which no fat thawing occurs, are targeted, and a smaller scan interval is being considered for more microscopic evaluation of various tissues.

Acknowledgment

This work was partly supported by KAKENHI 23H03758 and Chiba University Institute for Advanced Academic Research.

References

1) T. Ogawa et al., Proc. Acoust. J. Spr. **3-11-7** p.1127-1128, (2018) [in Japanese].
2) T. Ohnishi et al., MiCCAI COMPAY 2018 Workshop, LNCS vol. **11039**, p.103-111 (2018)

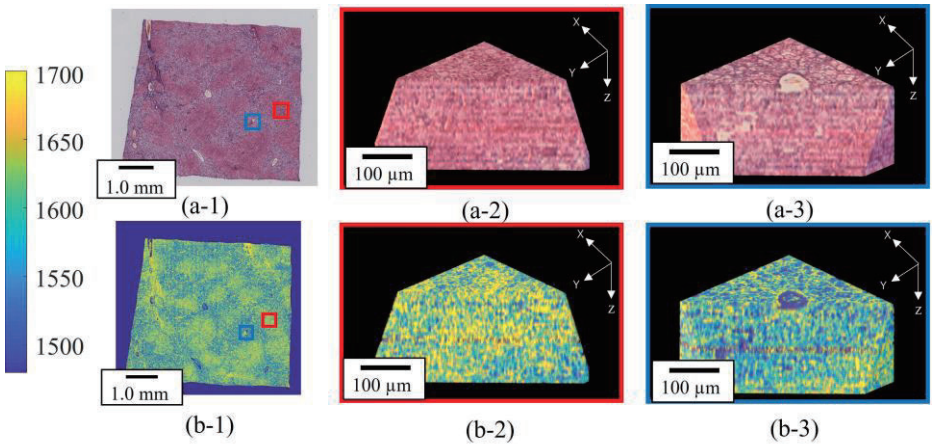

Fig. 1 Three-dimensional images of pathology and speed of sound in rat liver.